


PipeInfer: Accelerating LLM Inference using Asynchronous Pipelined Speculation

[1]Branden Butler, [1]Sixing Yu, [2]Arya Mazaheri, [1]Ali Jannesari
Iowa State University[1]
Technical University of Darmstadt[2]
{*butler1, yusx, jannesar*}*@iastate.edu, arya.mazaheri@tu-darmstadt.de*

***Abstract*—Inference of Large Language Models (LLMs) across computer clusters has become a focal point of research in recent times, with many acceleration techniques taking inspiration from CPU speculative execution. These techniques reduce bottlenecks associated with memory bandwidth, but also increase end-to-end latency per inference run, requiring high speculation acceptance rates to improve performance. Combined with a variable rate of acceptance across tasks, speculative inference techniques can result in reduced performance. Additionally, pipeline-parallel designs require many user requests to maintain maximum utilization. As a remedy, we propose PipeInfer, a pipelined speculative acceleration technique to reduce inter-token latency and improve system utilization for single-request scenarios while also improving tolerance to low speculation acceptance rates and low-bandwidth interconnects. PipeInfer exhibits up to a 2.15× improvement in generation speed over standard speculative inference. PipeInfer achieves its improvement through Continuous Asynchronous Speculation and Early Inference Cancellation, the former improving latency and generation speed by running single-token inference simultaneously with several speculative runs, while the latter improves speed and latency by skipping the computation of invalidated runs, even in the middle of inference.**

***Index Terms*—large language models, inference, speculation, acceleration, distributed, parallel**

I. Introduction

Large Language Models (LLMs) have become wildly popular in recent times, especially due to their versatility in tasks like language understanding and generation. Among the various architectures, decoder-only Transformer models like OpenAI's GPT series [1] and Meta's Llama family [2] have gained prominence. These models are comprised of a series of decoder layers, each of which is architecturally identical, sandwiched between an input embedding layer and an output layer [2], [3]. Unlike encoder-decoder models, decoder-only models focus solely on generating output sequences based on the input they receive. During inference, each layer feeds its outputs directly to the inputs of the successive layer. Their autoregressive nature means that for generating each output token, all layers need to be evaluated iteratively. This design introduces a significant challenge, as the model size exceeds the cache size of the target processor, and a memory bandwidth bottleneck becomes evident [4], [5]. This bottleneck impacts the model's scalability and processing speed, posing challenges in real-time applications.

Despite these challenges, the autoregressive approach is preferred for certain applications due to its ability to maintain high levels of accuracy and contextual understanding in sequence generation. Current research is actively exploring solutions to mitigate these bottlenecks, including advancements in hardware design [6], more efficient architectures [7], and novel parallel processing techniques for exploiting batched inference [8]. Batched inference is less susceptible to bandwidth limitations because of increased temporal and spatial locality, improving processor cache hit rate at the expense of increased latency.

Recently, innovative techniques aimed at mitigating the memory bandwidth bottleneck in LLMs have emerged, drawing inspiration from the concept of CPU speculative execution, including SpecInfer [8] and Staged Speculative Decoding [9]. These techniques use a smaller secondary model to generate a tree of speculative sequences, that are then batched together and run through the target model. The key to this process is that inferencing on a tree of speculations yields probability distributions for all tokens within the tree, allowing inference to jump ahead several tokens at a time. The speedup shown by these techniques is due to the greater efficiency that batched processing yields. Building on this concept, other techniques like Medusa [10] and Lookahead Decoding [11] have emerged, which adapt the speculative decoding approach by modifying the generation and verification of speculations.

A significant challenge with these speculative techniques is the latency escalation, particularly evident in scenarios of low speculation accuracy. The crux of the issue lies in the balance between computational time and effectiveness. Although each inference run may take longer, the efficiency is substantially compromised if the speculation accuracy is low, leading to fewer correct and verified tokens. This imbalance results in the computational and time costs outweighing the benefits gained from correct speculations. Additionally, in heterogeneous systems such as smartphones with CPUs, GPUs, and NPUs, synchronization costs are too high to make full utilization of all processing elements. Speculation techniques can partially resolve this by running speculation on one processing element and verification on another, but current methods only run one phase at a time and thus still show limited utilization.

In this paper, we rectify these issues by modifying the speculative inference algorithm to run multiple verification runs simultaneously, exploiting a pipeline-parallel architecture to achieve high system utilization while maintaining low communication overhead. Our design achieves remarkable

SC24, November 17-22, 2024, Atlanta, Georgia, USA
979-8-3503-5291-7/24/$31.00 ©2024 IEEE

resilience to interconnect and computation latency, enabling high-speed inference on low-cost clusters of disparate commodity hardware. We believe future work can build on our design to achieve higher utilization in heterogeneous systems despite interconnect latency and large throughput differences. Finally, our design is not bound to the speculative inference algorithms. We believe that this approach can be extended to other acceleration techniques, such as Lookahead Decoding or Medusa speculation heads.

Compared to pipeline-parallel speculative inference, we observe roughly a 1.5-2.15× improvement in overall generation speed in our test cases while achieving near-zero slowdown for poor speculation accuracy. Testing with Gigabit Ethernet as the interconnect revealed a tolerance to latency and throughput limitations, increasing its improvement over speculative inference in such scenarios. For well-aligned models, we observed up to 1.7× faster generation speed than pipeline-parallel speculation, and for poorly aligned models, we observed up to a 2.15× improvement.

We introduce several key contributions to the field of speculative decoding in large language models:

- **Asynchronous Speculation and Inference:** We enhanced speculative inference by integrating physically separate compute pipelines to run single-token inference or tree verification concurrently with the generation of the speculation tree. This modification enables simultaneous processing, significantly improving computational efficiency and reducing latency. Time-to-first-token latency reached near-parity with non-speculative iterative inference, while system utilization doubled.
- **Continuous Speculation:** By leveraging asynchronous speculation, we devised a method of continuously generating speculations in small micro-batches rather than large single batches, improving the end-to-end latency and reducing the penalty for low speculation acceptance rates. With continuous speculation, we observed that the latency reduction was directly proportional to the reduction in batch size. We also observed continuous speculation allowed PipeInfer to adapt to low-bandwidth scenarios. Continuous speculation improved PipeInfer's generation speed up to 1.5×.
- **Pipelined KV Cache Multibuffering:** To preserve the causality relationship of the generated tokens, we segmented the KV cache sequences into private sections for each speculative run. Cache operations are pipelined to maintain coherence during inference, allowing speculative runs to avoid computation of tokens shared by previous runs, even before they have been completed. By exploiting this ability, we improved computation throughput by a factor proportional to the alignment of the speculative model.
- **Early Inference Cancellation:** We devised a method of flushing invalidated runs from the pipeline by back-propagating an asynchronous cancellation signal, reducing the performance impact of continuous speculation with poorly aligned speculation models. Somewhat counter-intuitively, we observed greater speedups up to 2.15× for poorly aligned models thanks to early inference cancellation.

II. Background and Motivation

Large Language Models based on the Transformer decoder architecture, including Llama 2 [2] and GPT [1], are built up from a series of decoder layers. Each decoder layer contains an attention module and a multi-layer perceptron [3]. The attention module calculates the scores for all tokens in the sequence, but the key and value vectors are oftentimes cached to prevent needless recomputation.

During inference, each decoder layer is evaluated in sequence, requiring the weights for the attention module and MLP to be loaded, as well as the relevant entries from the KV cache. The sheer size of most modern models necessitates multiple gigabytes of memory transfers during a single inference run, resulting in a memory bandwidth bound for small batch sizes [9]. This bandwidth limitation mirrors similar constraints in CPU pipelines, causing significant stalls as the processing elements wait for values from memory [4]. Inspired by CPU speculative execution, many similar designs for speculative inference were created to alleviate this bottleneck [8]–[10].

A. Speculative Inference

Speculative inference operates through two principal components: the speculation phase and the verification phase.

1) Speculation: The speculation phase involves a set of secondary models paired with the primary target model. The secondary models are chosen to be smaller and faster to run than the primary target model. The speculative models are first run on the input sequence, generating multiple output sequences iteratively. They persist in this process until the highest output probability drops below a designated threshold that signifies the lowest confidence allowed for a speculative token. Upon achieving this cutoff, the comprehensive tree of speculative sequences, encompassing all potential outputs derived so far, is prepared for the next stage.

2) Verification: The verification phase takes the entire speculated tree and generates a special attention mask to ensure that sequences within the tree remain mutually exclusive in terms of their token visibility. This masking technique preserves causality relationships inherent in the sequences, while preventing any cross-interference amongst them.

Following this, the speculated tree and its corresponding attention mask are integrated into the target model's inference pipeline. When multiple tokens are fed into the inference pipeline, the output is a set of logit vectors for every token in the input tree. The verification phase then uses these vectors to iteratively compare the speculated tokens against the probability distribution of the target model at that token's position. If the speculated token matches a token that would have been sampled from the distribution, the verification phase accepts the speculated token and continues verifying other tokens in that sequence. Conversely, a mismatch leads to

sampling a new token from the probability distribution and then ends the verification.

Running a verification pass is more efficient than running each token through the entire model. The batch processing approach allows for the reuse of layer weights, reducing the frequency of CPU cache evictions. Additionally, the speculative inference mechanism includes a set of predictive probabilities for every leaf node in the speculative tree. These probabilities are leveraged to anticipate the next token for sequences that are entirely correct, ensuring that the target model inference is constantly productive, avoiding scenarios where a run is rendered completely pointless.

B. KV Cache

Upon completion of the verification phase, the system must modify the KV cache for both the target and the speculative models. The KV cache is a method of improving generation speed by caching attention vectors for previous tokens [3]. Entries corresponding to rejected tokens must be removed or otherwise masked in subsequent verification runs. Popular implementations, such as llama.cpp [12], attach metadata to each KV cache cell, identifying the entry's position and which sequences it belongs to. Such implementations perform the required cache modifications by modifying the metadata instead. The metadata is then used to construct the attention mask.

C. Challenges of Speculative Inference

In standard speculative inference, a notable bottleneck arises from the requirement that the target model's inference must wait until the completion of speculated sequences generated by the speculative models. This waiting period imposes a substantial delay on the time-to-first-token latency, a critical measure of system responsiveness. Additionally, the complexity and size of the speculative models were limited. Any increase in the inference latency of these speculative models has a direct and proportional effect on the latency of the entire system.

Existing work [8] also assumed that the speculative models were run on the same systems as the target model, requiring either significant GPU VRAM or significant number of nodes to split the target model weights between. At any given moment, only one set of these weights is actively utilized, suggesting the theoretical feasibility of temporarily paging them out to CPU RAM or disk space as needed. However, this approach introduces its own set of challenges and inefficiencies, especially in terms of resource management and access times. The trade-off here lies in balancing the requirement for rapid access to these weights against the limitations imposed by hardware resources, particularly in scenarios where VRAM or computational nodes are at a premium. We solve this issue by moving the speculative models to a dedicated pipeline, enabling further optimizations such as asynchronous speculation.

III. Related Work

Speculative decoding has previously been explored through SpecInfer [8] and Staged Speculative Decoding [9].

SpecInfer utilized multiple speculative models executed in parallel with each other, but did not run the speculative and target models in parallel, resulting in increased end-to-end latency. Staged Speculative Decoding took a slightly different approach, where the speculative models were themselves speculatively inferenced, improving overall speed but incurring even greater latency penalties, as the staged speculations were also not run in parallel with their respective targets.

Medusa [10] takes a slightly different approach to speculative decoding, adding new sampling heads to the target model that produce the speculations without a secondary model. Medusa does not incur significant latency overhead but requires training new sampling heads for the target model.

Lookahead Decoding [11] takes a different approach entirely, opting to use Jacobi iteration to generate multiple tokens simultaneously by generating N-grams based on the trajectory of the current tokens. The generated n-grams are cached and later verified in a separate stage. Lookahead Decoding exhibits high utilization and low latency on single-node systems, but does not account for multi-node systems or systems with slow interconnects.

A recent work named SPEED [13] uses similar speculative techniques to enhance decoding efficiency, but instead targets inference on a single GPU. Additionally, SPEED generates the speculations from the hidden states of previous layers, eliminating the need for a separate speculative model. This approach contrasts with PipeInfer, which utilizes a secondary model for speculation generation. While this difference impacts the computational overhead, it also influences the flexibility and adaptability of the system to different modeling scenarios. Moreover, invalidation of speculations results in a pause for the entire system in SPEED, while PipeInfer continues inferencing all other valid runs at the same time invalidation and flushing operations are executed. Finally, SPEED targets specialized models implementing parameter sharing, while PipeInfer works across a variety of off-the-shelf models.

Exploiting pipeline parallelism to improve inference latency while simultaneously running speculation has been explored previously [14]. However, this work performed speculation via similar methods to SPEED, predicting a single next token from the hidden states of intermediate layers, requiring additional sampling heads to be trained. Additionally, this method only speculates one token in advance at a time, limiting the possible speedup compared to other methods utilizing separate speculative models or heads.

Work has also been done using tensor parallelism, distributing the sub-layer operations across the nodes instead of whole layers [15]. However, such methods have been found to suffer from extreme interconnect bandwidth bottlenecks, even for extremely slow compute nodes like Raspberry Pi 4s. Even as few as eight nodes incurred higher synchronization time than the time spent running the inference itself.

Non-speculative techniques have also been explored in the area of inference acceleration. A prominent technique is based around early exit inference, in which some later model layers

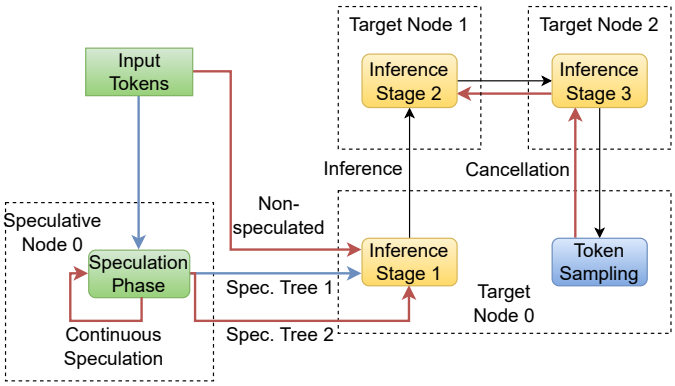

Fig. 1: High-level system architecture of PipeInfer. Changes from speculative inference are in red.

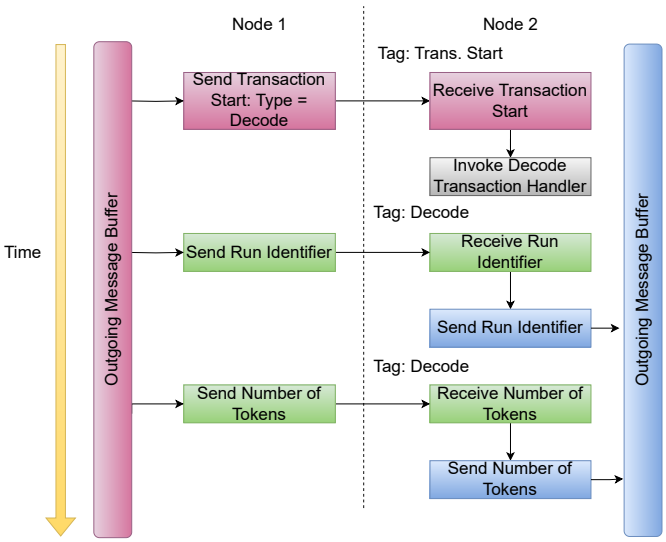

Fig. 2: Pipeline communication timeline.

are skipped if the output from an earlier layer can be used instead. CALM [16], for example, trains a classifier model to detect when an earlier layer is sufficiently confident in its output. Similarly, Depth-Adaptive Transformers [17] utilize classifiers to predict the depth at which inference can halt, either per-token or per-sequence. Yet another early-exit style strategy called LITE [18] accelerates inference while maintaining output accuracy, a problem that plagues other similar systems. Early exit decoding shows promise but requires training classifiers for the target model.

Other non-speculative acceleration techniques focus on modifying the precision at which inference is conducted. Such techniques include quantization strategies like AWQ [19] and QuIP [20] or pruning strategies like SparseGPT [21] and SparseML [22]. Still other techniques such as SqueezeLLM [23] combine sparsity and quantization. Quantization and pruning approaches generally require an offline conversion step to compress the original model weights but can be substantially less intensive than a full pre-training run.

PipeInfer does not require any pre-training or conversion steps, but also does not conflict with quantization or pruning techniques.

IV. PipeInfer Method

Our proposed method, PipeInfer, enhances speculative inference and is composed of four major components: Asynchronous Speculation, Continuous Speculation, Pipelined KV Cache Multibuffering, and Early Inference Cancellation. Our reference implementation is built on top of llama.cpp [12], with inter-node communication accomplished with MPI [24]. An overall system diagram is shown in Figure 1.

A. Asynchronous Speculation

Requiring the target model inference pipeline to wait for the speculative sequences to be generated increases both the time-to-first-token (TTFT) latency and the inter-token latency. PipeInfer reduces these latencies through Asynchronous Speculation, in which the target pipeline runs in parallel with speculation. To accomplish this, PipeInfer utilizes two loosely coupled compute pipelines, one for the target model and one for the speculative model. After the initial prompt processing, both pipelines are fed the first generated token. The target pipeline runs inference on this single token, while the speculative pipeline generates a tree of speculative sequences. Once the speculative tree is completed, it is fed into the target pipeline, which performs verification of the tree. Upon completion of the first inference run, the logits are transferred to the head node, which performs sampling, and the process repeats.

For greater speculation accuracy, larger speculative models may be used without drastically increasing the inference latency of the system because of the asynchronous design: a larger speculative model requires more time to generate the speculation tree, but the target pipeline is simultaneously running inference. Multiple speculative models may also be used, with varying sizes such that the smallest and the least accurate speculative model quickly generates a speculation tree to keep the target pipeline full, while the largest speculative model generates a more accurate tree.

1) State tracking: Each run of the target pipeline is tracked in a data structure containing the computation graph, the batch used to start the run, and an array of indices mapping each token in the batch to the corresponding set of logits. The data structure is created immediately before the run starts and placed in a FIFO queue. When the run starts, the head node sends configuration data down the pipeline, detailing information such as the batch size and the array of sequences per token. The head node then evaluates the first few layers according to the allocated split. Once finished, the activation tensors are sent to the next node. All send operations are completed using a buffered implementation, enabling a sending node to continue before the receiving node is ready.

2) Pipeline operation transactions: Most pipeline operations, such as sending configuration data or activation tensors, are strictly ordered so that activation tensors cannot be

received before the requisite configuration data is received and processed. PipeInfer accomplishes this using MPI tags: a start message indicates the beginning of a transaction, a construct defined by PipeInfer to indicate a single atomic operation that must be executed in the same order as received. The transaction start message contains the tag identifying the transaction type, and a handler on each worker node invokes the function corresponding to that type. All MPI send and receive calls within said function use the tag attributed to the transaction type. MPI point-to-point communications are non-overtaking for messages with the same sender, receiver, and tag [24], so in this way, we guarantee deterministic ordering of pipeline transactions. This process is shown in Figure 2.

B. Continuous Speculation

Asynchronous speculation improves end-to-end latency, but there is still significant under-utilization in the single-request scenario. After the speculative tree is generated, much of the system remains idle until the target pipeline completes the initial non-speculative run. This is not a problem for short pipelines as the system utilization is proportionally higher, but longer pipelines suffer from large bubbles of inactivity.

Continuous Speculation reduces the size of these bubbles by generating speculative trees whenever the head node would otherwise be idle. The idle state is determined by probing for an incoming logits transfer transaction. If a transaction is waiting to be processed, the head node invokes the sampling and verification routine. Otherwise, the node generates another speculation tree. By opportunistically generating speculations, system utilization improves proportionally to the pipeline depth. A timeline of continuous speculation is shown in Figure 3.

Speculative trees generated in this fashion build on the previous trees, so if an earlier speculation is rejected, many speculative runs are invalidated.

1) Microbatching: An immediate problem with continuous speculation relates to the size of the speculated trees. In standard speculative inference and asynchronous speculation, larger trees have the potential to improve generation speed over smaller trees, as larger batches incur fewer CPU cache misses and less inter-node communication compared to multiple smaller batches. However, the size of the speculative tree proportionally increases the inference latency. Additionally, as the depth of the tree increases, the probability of an entire sequence being accepted decreases due to the divergence between the speculative and target model outputs. Therefore, larger batches may incur higher latency without improving the number of accepted tokens.

This same principle applies to continuous speculation but is magnified by the greater number of speculative runs. As a counter-balance, Pipeinfer generates micro-batches of speculations, ranging from 1 to 4 tokens in size. The smaller batch size improves inference latency at the cost of increased memory bandwidth pressure. The benefit of micro-batches is three-fold: (1) the imbalance between speculative and non-speculative runs is reduced, decreasing the size of inactivity bubbles related to this imbalance; (2) splitting a large speculative batch into many micro-batches allows the system to update the speculative model's known-correct tokens after verification of only a single micro-batch, improving the overall acceptance rate; (3) micro-batches enable finer granularity in the context of Early Inference Cancellation, another component of PipeInfer. Microbatching improves overall inter-token latency, run-to-run latency jitter, token acceptance rates, and system utilization.

2) Reactive speculation: As the number of speculation trees grows, the probability of all tokens being accepted drops, as the sequences eventually diverge from the target model. As an attempt to prevent wasted computation, we added another parameter to continuous speculation called the confidence cutoff recovery factor. This recovery factor is a floating point value added to the original speculation confidence cutoff for every successful iteration of continuous speculation, reset upon acceptance of a completed run. The effect is that of an increasing gradient of required confidence to continue speculation, reducing the probability of wasted computation.

We also added the inverse, the confidence cutoff decay factor, which is subtracted from the cutoff threshold when speculation fails and no logits are waiting to be sampled. This decay factor is designed to increase utilization when waiting for the rest of the pipeline to complete.

With these two factors, PipeInfer's continuous speculation becomes adaptive to system conditions in real-time, reacting to unexpected slowdowns gracefully and scaling both up to high-performance university-grade clusters and down to consumer-grade Beowulf clusters. These factors also allow for PipeInfer to be tuned towards higher performance or greater power efficiency.

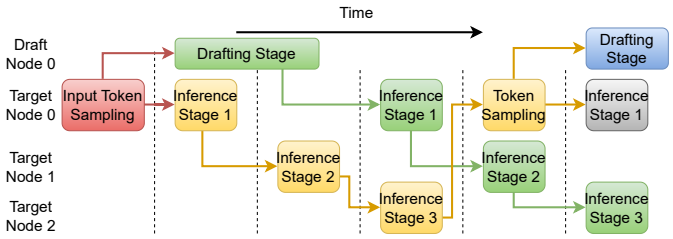

Fig. 3: The timeline of PipeInfer using continuous asynchronous speculation.

C. Pipelined KV Cache Multibuffering

Running multiple speculations and a non-speculative inference simultaneously requires careful management of the KV cache, the mechanism by which attention-related vectors are cached to prevent needless recalculation. PipeInfer uses the KV cache implementation present in llama.cpp [12]. The cache metadata enables near-zero slowdown from copying large numbers of cache cells from one sequence to another. PipeInfer uses this design to create multiple partitions of sequence ranges, each range dynamically allocated on a FIFO policy to a particular inference run. A queue stores the currently free

sequence identifiers, which designate the beginning of such a range.

1) Sequence partitions: PipeInfer runs non-speculated inferences using a pre-determined sequence identifier of zero, termed the canonical sequence, while speculated inferences are allocated a sequence identifier from the aforementioned FIFO queue. Combined with the causal attention mask, each inference run is guaranteed to not interact with cache entries from other inference runs.

The partitions act similarly to the back and front buffers in common double-buffering schemes: while a speculative run is in progress, the partition acts as the back buffer, only being readable by the assigned inference run. Once a speculative run is completed, a "buffer swap" is performed, where entries corresponding to accepted tokens are copied to the "front buffer", and the partition is marked as free for use by other runs. The front buffer in this analogy is the canonical sequence.

2) Sequence acceptance and propagation: When a speculated sequence is accepted during verification, the cache entries for that sequence are additionally copied to all other sequences, ensuring that new runs have the correct entries. Only the entries up until the position of the final accepted token are copied, ensuring that the cache entries of in-progress runs are not altered beyond what has already been accepted. Overwriting existing entries in allocated partitions would cause correctness issues if the entries were modified before the attention values had been calculated, potentially causing race conditions and incorrect output. PipeInfer carefully manages operation ordering to prevent such conditions from occurring.

3) Transactions and early cache entry sharing: Cache operation commands are not broadcast to all nodes simultaneously but are pipelined like the activation tensors, using the same transaction mechanism. Doing so ensures the integrity of in-progress runs and allows PipeInfer to immediately send a cache copy command after beginning inference of a non-speculated run, resulting in the guaranteed-correct cache entries being copied to all sequences immediately after a node is finished evaluating its set of layers. Copying these entries enables speculated runs to skip evaluation of the first token in a sequence and, instead, reuse the cache entry for that token.

D. Early Inference Cancellation

When running multiple inferences simultaneously, there is a chance that by accepting multiple tokens in token-tree verification, some runs in the pipeline become superfluous or invalid. Invalidation occurs when a speculative run in the pipeline has beginning tokens that do not match what has been accepted, meaning all tokens in the run are guaranteed to be rejected. Superfluous runs occur when all tokens in the run are already accepted; for example, a non-speculative run may become superfluous if a previous speculative run had also generated the same token.

1) Invalidation detection: PipeInfer detects these scenarios through two methods: comparing a run's starting and maximum ending token positions against the current accepted tokens' end position, and comparing each run's token sequences against the currently accepted tokens. Both methods use a data structure containing the speculated tokens and the run's maximum and minimum token positions. This data structure is created when a run is begun and placed in a FIFO queue. In the former method, if the maximum end position of a run is less than the current accepted tokens' end position, then the run is marked as superfluous. In the latter method, the head node loops over the FIFO queue after every sampling phase and compares the speculated tokens against the currently accepted tokens. If the beginning of the speculated sequence does not match the end of the accepted tokens, then the run is marked as invalidated.

2) Cancellation back-propagation: Upon detection of superfluous or invalidated runs, PipeInfer back-propagates a special cancellation signal through the pipeline. The signal contains only a uniquely assigned identifier corresponding to the run that should be canceled. Nodes that have not yet evaluated the canceled run will skip the evaluation entirely, improving performance when the pipeline is saturated or if there is a slower node that would otherwise become a bottleneck. Nodes currently evaluating a run probe for a cancellation signal at thread synchronization points, allowing a node to skip computation even while it is currently processing the canceled run.

Upon completion of a run, the data structure containing its speculated tokens and their positions is popped from the FIFO. To maintain consistency, canceled runs still transfer empty activation tensors down the pipeline, so the ordering of messages is maintained, and the internal state of each node is kept intact. Therefore, canceled runs still incur a small amount of communication.

3) Performance considerations and conflicts: Early Inference Cancellation only improves performance when canceling speculated runs; non-speculated runs are marked as canceled but are still evaluated in their entirety, and only final sampling is skipped. The reason behind this difference in behavior is the fact that Pipelined KV Cache Multibuffering relies on the fact that non-speculated runs are always evaluated in their entirety to skip the evaluation of the first token in a speculated run. If non-speculated runs were indeed canceled mid-stream, the subsequent cache-copy commands would copy invalid entries into the speculated run's sequence partition.

E. Model Accuracy

PipeInfer accelerates the inference procedure without any loss of model accuracy. At the sampling and token verification stage, each speculated token is only accepted if it can be verified that sampling from the target model's output distribution would have yielded that token. We use the token verification algorithm from SpecInfer [8] for this stage.

For the token verification algorithm to guarantee the same model output as in the non-speculative naive inference mode, the output probability distribution from the model must also be the same. PipeInfer's careful management of the KV cache guarantees that each simultaneous speculative inference run is

entirely independent, and the use of transactions guarantees the correct order of operations.

Early inference cancellation only cancels runs that are guaranteed not to be accepted, and all other runs are allowed to be completed. Non-speculative runs are always allowed to run to completion, guaranteeing the KV cache is kept in a consistent and valid state.

V. Experiments

A. Experiment Setup

Testbed. We evaluate the performance of PipeInfer by running various LLMs on various compute nodes with different configurations. The cluster configurations are shown in Table II. On multi-socket systems, NUMA awareness was enabled, and the model weights were distributed among the NUMA nodes to take advantage of the independent memory channels. The 13 heterogeneous nodes comprised five old Dell Optiplexes in combination with 8 Intel Xeon nodes. This configuration was used to test the resilience of PipeInfer to heterogeneous pipelines, where slower nodes could stall the pipeline due to greater computation or memory bandwidth bottlenecks. The Optiplexes were configured with second- and fourth-generation Intel Core i5 and i7 processors, all five of them utilizing dual-channel DDR3 memory.

On cluster C, experiments were executed via a job manager and given exclusive access to all nodes. On clusters A and B, no job manager was present, and only essential system services were running.

Tested Prompts. The prompts we tested with were 128 tokens long, formatted according to the models' expected prompt formats. We used multiple prompts to test different usage scenarios and to align with each model's expected use case:

- The first prompt asked the model to generate a Python program that demonstrates advanced features, asking it to withhold any explanation, so the model generates only code.
- The second prompt asked the model to write a fictional tale about a warrior named Goliath.
- The third prompt used no special formatting and was a randomized excerpt of the Wikitext-2 dataset [31].

All the models generated 512 output tokens using greedy sampling. We opted to use greedy sampling to maintain the exact generations across all three inference strategies.

Model Pairs. The LLM model pairs involved in our experiments are shown in Table I, including the Llama [2] and Falcon [30] model families, as well as a popular Llama merge called Goliath [28]. Goliath is a unique model created by splicing two Llama 2-70B models together, resulting in a tall and thin model architecture compared to Falcon, which is wider. We added Goliath to our test cases to determine whether elongated architectures favor one inference strategy disproportionately over others.

Baselines. We compare PipeInfer with standard, iterative inference in a pipeline-parallel scenario as well as pipeline-parallel speculative inference, which is an implementation of SpecInfer [8] using a single speculative model.

Evaluation metrics. We recorded four primary metrics during our experiments:

1) **Average generation speed** is measured by recording the total wall clock time between the beginning and completion of inference, not accounting for initial prompt processing and prefilling.
2) **Time-to-first-token latency (TTFT)** is measured as the CPU time consumed by the main thread between the completion of the prompt processing phase and the first token acceptance, not including the token sampled at the end of prompt processing. We do not consider the token sampled from the prompt processing stage as the first token because not all inference scenarios require a prompt processing stage, such as when the prompt is cached, and because neither speculative inference nor PipeInfer are engaged during prompt processing.
3) **Inter-token latency (ITL)** measures the average time between each accepted token. ITL measurements were taken by recording the CPU time consumed by the main thread in between each accepted token and averaging the recordings. It should be noted that ITL measures the time between each token acceptance and not the time between starting and completing a run.
4) **Per-node memory consumption** was recorded through pmap [32]. Model files were memory-mapped, and only the pages that incurred a page fault on the node were included in the memory usage calculations. Before each experiment, we cleared the file cache to guarantee that pages were faulted into the memory attached to the same socket that requested the data, ensuring a consistent experimental environment.

We also observed the output directly and compared it against the single-node inference baseline output to evaluate correctness. This was possible because the decision to use greedy sampling ensured deterministic output with no run-to-run variance in generated output for a given input prompt.

B. Experiment Results

For evaluation, we implemented PipeInfer on top of the popular Llama.cpp framework [12]. The framework includes both a reference implementation for speculative inference and for standard, single-node inference. The framework also includes an implementation of pipeline-parallel inference using MPI.

To measure the improvement of PipeInfer, we ran inference of several models in four scenarios: normal single-node inference, naïve pipeline parallel inference, pipeline-parallel speculative inference, and PipeInfer inference. We ran each experiment 10 times and averaged the results. Unless otherwise specified, all experiments were run on the Intel Xeon Gold compute nodes.

Generation speed analysis. The Dolphin and TinyLlama pair exhibited acceptance rates of approximately 79% with the speculative tree size capped at four tokens; the resulting generation speeds are shown in Figure 4a. We observed that PipeInfer improved generation speed over speculative and iterative inference in all recorded test cases. We also observed

TABLE I: List of target models paired with speculation models.

Target Model	Size	Quantization	Architecture	Speculative Model	Size	Quantization	Architecture
Dolphin 2.1 [25]	70B	Q3_K_M	Llama 2	TinyLlama OpenOrca [26] Orca 2 [27]	1.1B 7B	Q4_K_M Q4_K_M	TinyLlama Llama 2
Goliath [28]	120B	Q2_K	Llama 2 Merge	XWinLM 0.2 [29] XWinLM 0.1 [29]	7B 13B	Q4_K_M Q4_K_M	Llama 2 Llama 2
Falcon Base [30]	180B	Q3_K_M	Falcon	Falcon Base [30] Falcon Base [30]	7B 40B	Q3_K_M Q3_K_M	Falcon Falcon

TABLE II: Hardware testbed specifications

Cluster Name	Max nodes	CPUs	RAM	Interconnect
A	8	2× Intel Xeon E5-2650	128GB 1600 MT/s DDR3	Gigabit Ethernet
B	13	Heterogeneous: 2nd and 4th Gen i5 and i7, 2× Intel Xeon E5-2650	8GB DDR3	Gigabit Ethernet
C	32	2× Intel Xeon Gold 6140	384GB 2666 MT/s DDR4	Infiniband EDR 100Gb/s

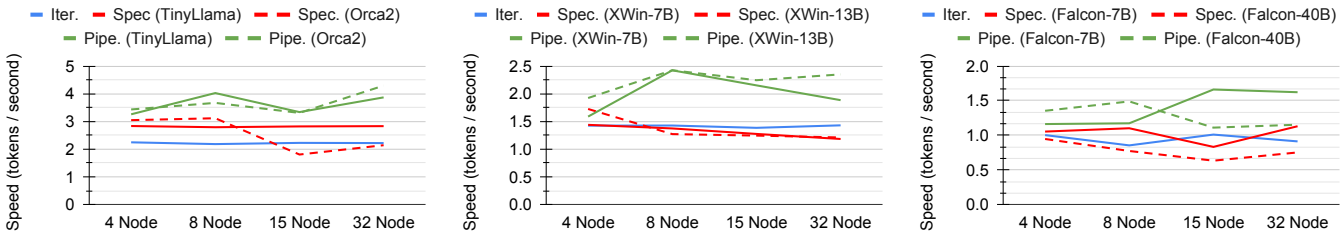

(a) Dolphin-70B speeds using TinyLlama or Orca2 speculative models.

(b) Goliath-120 speeds using XWinLM-7B or XWinLM-13B speculative models.

(c) Falcon-180B speeds using Falcon-7B or Falcon-40B speculative models.

Fig. 4: Generation speeds of model pairs using different inference techniques.

that generation speed using speculative and iterative inference was essentially constant as the number of nodes increased. We believe this is due to a combination of the extremely fast interconnect and the target model activation tensors being relatively small.

Switching TinyLlama for Orca 2 7B curiously decreased the overall acceptance rate to 66%, decreasing performance for iterative and speculative inference, as shown in Figure 4a. PipeInfer instead shows similar performance to the TinyLlama tests, with slight improvements in the 8 and 32 nodes cases. We observed that the speculative inference case no longer exhibited constant generation speed as the number of nodes increased; we theorize that Orca2's confidence in its speculations was high enough to produce larger speculative trees per run, while not aligning well enough with the target model to substantially reduce the number of runs required, resulting in increased interconnect bandwidth pressure.

Compared to the Dolphin pairs, the Goliath and XWin-7B pair produced an exceptionally low acceptance rate of 52%, causing a decline in the performance of speculative inference as the number of nodes increased. Figure 4b plots this decline. PipeInfer's resilience to low alignment is again demonstrated, achieving significantly higher generation speeds than the other two inference strategies. The highest generation speed was attained at eight nodes, followed by a slow decline in performance as the number of nodes increased.

To test whether the acceptance rate affects the optimal number of nodes, we replaced XWin-7B with XWin-13B, improving the acceptance rate to 61%. Figure 4b reveals that while enhanced alignment increased generation speed, it did not alter the optimal node count, which remained at 8. We did observe that the 32-node configuration reached parity with the 8-node configuration, while the 15-node configuration only marginally improved over the XWin-7B test, suggesting non-linearity in the scaling of PipeInfer.

Falcon-180B, paired with Falcon-7B, had a high acceptance rate relative to the size disparity of the models: 68.675%. Figure 4c reveals that, with a sufficiently high acceptance rate and sufficiently low speculative model size, speculative inference approaches the performance of PipeInfer for low numbers of nodes. However, as the number of nodes increases, PipeInfer's performance spikes while speculative inference's generation speed drops.

Increasing the acceptance rate to 69.47% by switching Falcon-7B with Falcon-40B reverses the trend: the difference between the two strategies is greatest at lower numbers of nodes due to the extreme computation requirements of the speculative model. Figure 4c shows this trend.

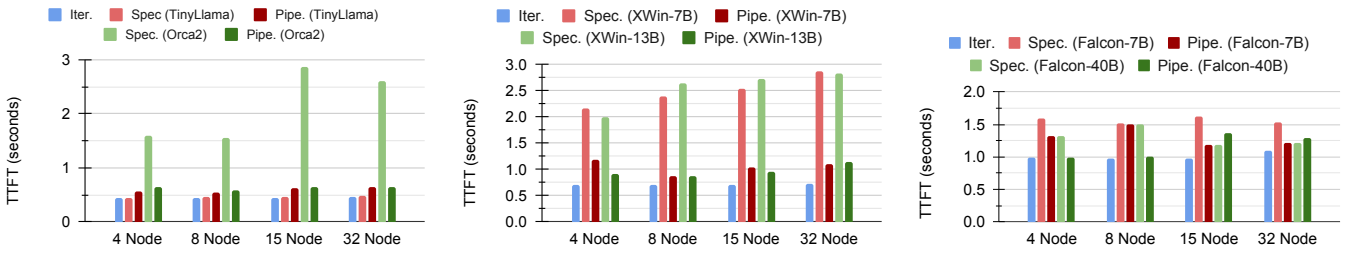

(a) Dolphin-70B paired with TinyLlama and Orca2

(b) Goliath-120B paired with XWin-7B and XWin-13B.

(c) Falcon-180B paired with Falcon-7B and Falcon-40B.

Fig. 5: Time-to-first-token (TTFT) latencies of model pairs using different speculative models.

Time-to-first-token latency analysis. Examining the time-to-first-token latencies of the previous tests reveals that PipeInfer achieves near-parity with iterative inference and substantially lower latencies compared to speculative inference. This is shown in Figures 5a, 5b and 5c. We observed that increasing the speculative model size did not noticeably impact the TTFT latency. PipeInfer, therefore, becomes an excellent fit for real-time or conversational scenarios. Speculative inference suffered drastically higher latencies as a consequence of waiting for the speculative trees.

Inter-token latency analysis. Figures 6a, 6b, and 6c show the inter-token latencies recorded during our experiments. We observed that the ITL measurements followed the trends shown by the measured generation speed, verifying the correctness of our results.

Memory efficiency analysis. Memory usage was recorded during each experiment. We observed that the memory consumption of PipeInfer was equal to that of speculative inference. Per-node memory usage was reduced for all inference strategies as the number of nodes increased. Iterative inference maintained lower memory requirements due to the lack of a speculative model.

Comparing the per-node memory usage with the generation speed in Figure 7a reveals that, of the three inference strategies, PipeInfer achieves the highest speed-to-memory-consumption ratio, indicating that PipeInfer scales down to low-end cluster configurations very well.

Constrained hardware performance analysis. To measure the effect of computation and bandwidth constraints, we ran several inference experiments on two more clusters, each using substantially slower hardware and Gigabit Ethernet interconnects, the results of which are shown in Figure 7c. PipeInfer exhibited its greatest speedups over speculative inference in this scenario, likely due to the increased cost of speculation and the adaptability afforded by early inference cancellation. We also observed that increasing the number of nodes improved performance in all but two cases, even if the new nodes were slower than the original ones. For the Dolphin pair, adding additional nodes beyond the 8 Xeon E5 nodes decreased performance only marginally, while in the Falcon case, performance was reduced substantially. We believe the steep decline for the Falcon case is a result of the large model size, exacerbating the computation bottleneck on the slowest nodes. The Goliath test showed improved performance with the slower nodes, and we believe this is due to the low acceptance rate combined with early inference cancellation and the unique tall and thin architecture.

An important observation we made is that PipeInfer appears less susceptible to performance degradation caused by low alignment: PipeInfer's improvement over speculative inference increased for Goliath compared to Dolphin and Falcon. Conversely, PipeInfer's improvement was marginal when deployed in shallow pipelines.

Testing on these lower-end clusters also showed the extreme latency improvement asynchronous speculation provides. The time-to-first-token latencies are shown in Figure 7b. In some cases, PipeInfer achieved lower TTFT latencies than iterative inference; this is attributed to the fact that one of the nodes is solely dedicated to speculation under PipeInfer, making the target pipeline one node shorter than in the iterative inference case.

Model output and accuracy. We verified that the output of PipeInfer was consistent with the output from standard speculative inference, pipeline-parallel iterative inference, and single-node inference. Our decision to use greedy sampling resulted in deterministic output for all cases, and we verified that there was zero deviation between PipeInfer's final output and the output of the other methods.

Ablation Studies. We performed several ablation studies with three different model pairs on an 8-node configuration of Cluster C. The results of the studies are shown in Figure 8. The baseline of PipeInfer with all features enabled is included for comparison purposes. Ablating early inference cancellation resulted in decreased generation speed and increased inter-token latency consistent with our hypotheses. Removing continuous speculation and increasing the speculative batch size as a counter-balance caused severe performance degradation for the Dolphin and Goliath models and moderate performance degradation for Falcon. We hypothesize that Falcon's greater resistance to this ablation can be attributed to early-inference cancellation canceling a significant percentage of continuously speculated runs. Ablating KV cache multibuffering resulted in incoherent output, and removing asynchronous speculation serialized all other operations, causing corruption of the KV

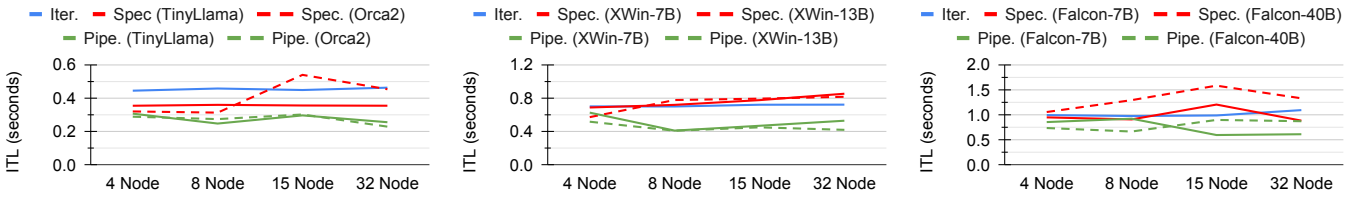

(a) Dolphin-70B paired with TinyLlama or Orca2.

(b) Goliath-120B paired with XWin-7B or XWin-13B

(c) Falcon-180B paired with Falcon-7B or Falcon-40B.

Fig. 6: Inter-token latencies (ITL) of model pairs using different speculative models.

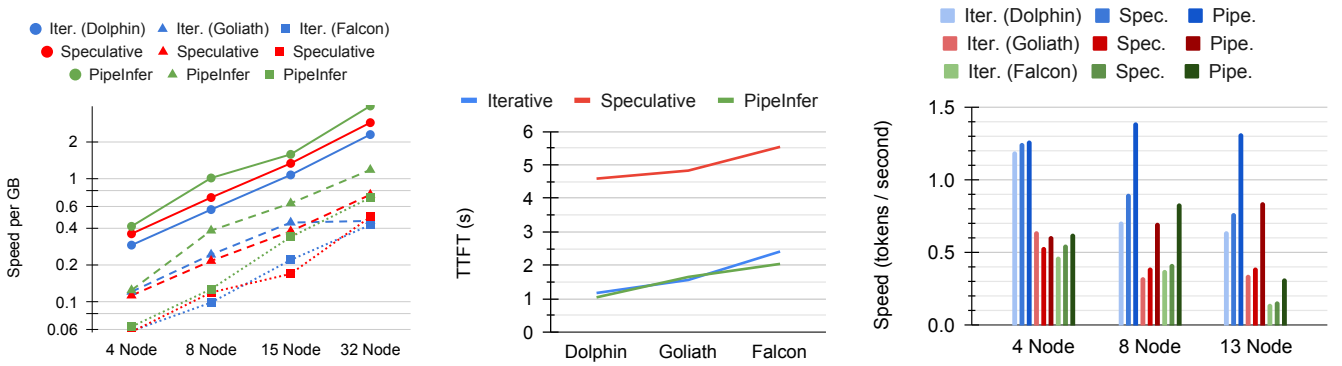

(a) Memory Efficiency. The Y axis is in logarithmic scale.

(b) TTFT under different inference methods and models on cluster A.

(c) Generation speeds of model pairs using small speculative models on constrained clusters.

Fig. 7: Resource and performance analysis on constrained hardware.

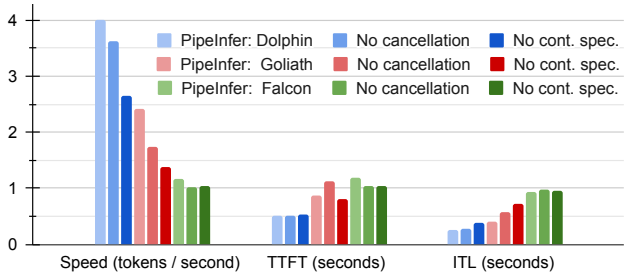

Fig. 8: Ablation studies on 8 nodes with Tinyllama, XWin-7B, and Falcon-7B as speculative models.

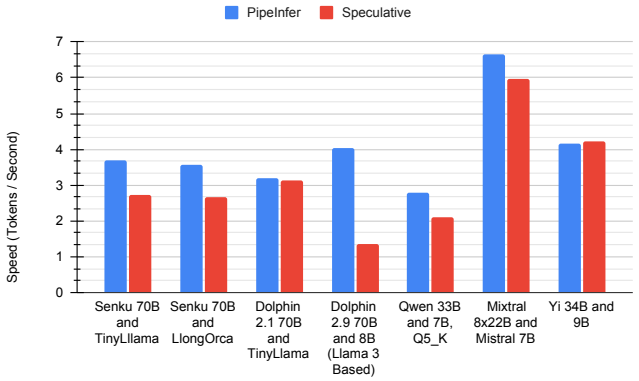

Fig. 9: Overall token generation speed on a 4-GPU cluster across many different model pairs.

cache and incoherent output. Therefore, we did not include performance numbers for these two ablations, since they experienced correctness errors.

VI. GPU Experiments

We have conducted experiments with PipeInfer using combined GPU and CPU computation. However, our GPU implementation is based on a later `llama.cpp` commit, after substantial backend refactoring, and so these results are not directly comparable with our previous CPU only results. Additionally, the MPI GPU implementation is not yet fully optimized and we expect continued improvement across the board in the future.

A. Experiment Setup

Testbed. Our GPU evaluation utilized a wide variety of hardware to test the effectiveness of our method across multiple GPU vendors and APIs. The testbench configuration is shown in Table IV.

We also tested with a large variety of model families, shown in Table III.

TABLE III: List of target models paired with speculation models.

Target Model	Size	Quantization	Architecture	Speculative Model	Size	Quantization	Architecture
Dolphin 2.1 [25]	70B	Q3_K_M	Llama 2	TinyLlama OpenOrca [26] Orca 2 [27]	1.1B 7B	Q4_K_M Q4_K_M	TinyLlama Llama 2
Senku [33]	70B	Q3_K_M	Llama 2	TinyLlama OpenOrca [26] LongOrca	1.1B 7B	Q4_K_M Q4_K_M	TinyLlama Llama 2
Dolphin 2.9 [25]	70B	Q3_K_M	Llama 3	Dolphin 2.9	8B	Q4_K_M	Llama 3
Qwen [34]	33B	Q5_K	Qwen	Qwen	7B	Q5_K	Qwen
Mixtral [7]	8x22B	Q3_K_M	Mixtral	Mistral	7B	Q4_K_M	Mistral
Yi [35]	34B	Q3_K_M	Llama	Yi	9B	Q4_K_M	Llama

TABLE IV: GPU testbed specifications

Number of nodes	CPUs	RAM	Interconnect	GPUs
4	2× Intel Xeon E5-2640 V3	128GB 1866 MT/s DDR4	Infiniband QDR 40Gb/s	AMD Instinct MI60, Nvidia Tesla P40, Titan V, RTX 3090

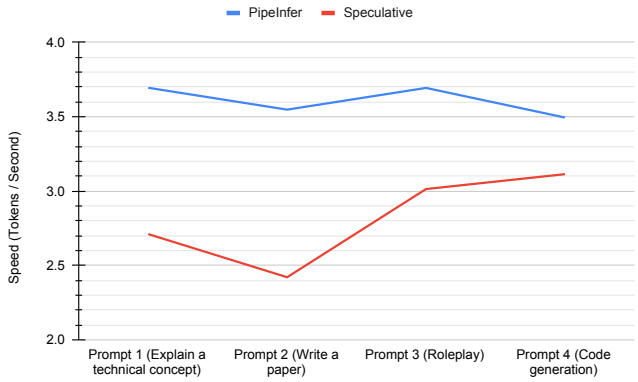

Fig. 10: Prompt-to-prompt variance using Senku 70B and TinyLlama 1.1B on a 4-GPU cluster.

B. Experiment Results

As shown in Figure 9, we observed similar patterns in our GPU results to our previous experiments. The overall generation speed of PipeInfer was greater than standard speculative inference in all but one case. However, we observed some significant outliers, specifically in the experiment involving the Dolphin 2.9 70B and 8B model pair. This pair is the only Llama 3-based pair we tested, thus we are unable to conclude whether this outlier is specific to Dolphin 2.9 or whether it is inherent to Llama 3 models in general.

We also included an additional set of experiments focusing on prompt-to-prompt variance, shown in Figure 10. In these experiments, we observed that PipeInfer's overall generation speed remained relatively consistent across the range of tested prompts, while speculative inference saw more erratic speed changes.

VII. Conclusion and Outlook

PipeInfer enhances the efficiency and processing speed of LLMs by modifying the speculative inference algorithm to support multiple verification runs within a pipeline-parallel architecture. We achieved not only optimized system utilization and minimized communication overhead but also demonstrated exceptional resilience to latency and computational delays, especially in cost-effective, heterogeneous hardware environments. The results show a remarkable 2.15× improvement in generation speed, maintaining high performance even with low speculation accuracy. Additionally, our approach exhibits robustness in latency and throughput-constrained environments, achieving high CPU and GPU utilization.

PipeInfer exhibits far-improved performance in multiple scenarios, and future work may extend it to other inference acceleration strategies, further improving its performance. We believe that Lookahead decoding [11] and Medusa [10] would benefit greatly from PipeInfer augmentation. We also believe self-speculation techniques like SPEED [13] or PPD [14] could complement PipeInfer's external speculative model approach.

PipeInfer may also be extended to support hybrid parallelization via multi-GPU nodes, applying tensor parallelism at the local node level and maintaining pipeline parallelism across the cluster. Alternatively, bandwidth bottlenecks resulting from the PCIe bus could be alleviated through the application of PipeInfer on a single node.

Bottlenecks in a pipeline can also be mitigated by adding new nodes in parallel with the slowest nodes, acting as load-balancers. When the primary node is busy, the secondary nodes can take over the computation of the designated layers. PipeInfer's use of many independent and simultaneous inference runs allows such load-balancing without affecting the end results, so long as the ordering remains consistent.

REFERENCES

[1] T. B. Brown, B. Mann, N. Ryder, M. Subbiah, J. Kaplan, P. Dhariwal, A. Neelakantan, P. Shyam, G. Sastry, A. Askell, S. Agarwal, A. Herbert-Voss, G. Krueger, T. Henighan, R. Child, A. Ramesh, D. M. Ziegler, J. Wu, C. Winter, C. Hesse, M. Chen, E. Sigler, M. Litwin, S. Gray, B. Chess, J. Clark, C. Berner, S. McCandlish, A. Radford, I. Sutskever, and D. Amodei, "Language models are few-shot learners," 2020.

[2] H. Touvron, T. Lavril, G. Izacard, X. Martinet, M.-A. Lachaux, T. Lacroix, B. Rozière, N. Goyal, E. Hambro, F. Azhar, A. Rodriguez, A. Joulin, E. Grave, and G. Lample, "Llama: Open and efficient foundation language models," 2023.

[3] A. Vaswani, N. Shazeer, N. Parmar, J. Uszkoreit, L. Jones, A. N. Gomez, L. Kaiser, and I. Polosukhin, "Attention is all you need," 2023.

[4] D. A. Patterson, "Latency lags bandwith," *Commun. ACM*, vol. 47, p. 71–75, oct 2004.

[5] N. Shazeer, "Fast transformer decoding: One write-head is all you need," 2019.

[6] S. Markidis, S. W. D. Chien, E. Laure, I. B. Peng, and J. S. Vetter, "Nvidia tensor core programmability, performance & precision," in *2018 IEEE International Parallel and Distributed Processing Symposium Workshops (IPDPSW)*, IEEE, May 2018.

[7] A. Q. Jiang, A. Sablayrolles, A. Roux, A. Mensch, B. Savary, C. Bamford, D. S. Chaplot, D. de las Casas, E. B. Hanna, F. Bressand, G. Lengyel, G. Bour, G. Lample, L. R. Lavaud, L. Saulnier, M.-A. Lachaux, P. Stock, S. Subramanian, S. Yang, S. Antoniak, T. L. Scao, T. Gervet, T. Lavril, T. Wang, T. Lacroix, and W. E. Sayed, "Mixtral of experts," 2024.

[8] X. Miao, G. Oliaro, Z. Zhang, X. Cheng, Z. Wang, R. Y. Y. Wong, A. Zhu, L. Yang, X. Shi, C. Shi, Z. Chen, D. Arfeen, R. Abhyankar, and Z. Jia, "Specinfer: Accelerating generative large language model serving with speculative inference and token tree verification," 2023.

[9] B. Spector and C. Re, "Accelerating llm inference with staged speculative decoding," 2023.

[10] T. Cai, Y. Li, Z. Geng, H. Peng, and T. Dao, "Medusa: Simple framework for accelerating llm generation with multiple decoding heads." https://github.com/FasterDecoding/Medusa, 2023.

[11] Y. Fu, P. Bailis, I. Stoica, and H. Zhang, "Breaking the sequential dependency of llm inference using lookahead decoding," November 2023.

[12] G. Gerganov, "ggerganov/llama.cpp: Port of facebook's llama model in c/c++." https://github.com/ggerganov/llama.cpp, 2023.

[13] C. Hooper, S. Kim, H. Mohammadzadeh, H. Genc, K. Keutzer, A. Gholami, and S. Shao, "Speed: Speculative pipelined execution for efficient decoding," 2024.

[14] S. Yang, G. Lee, J. Cho, D. Papailiopoulos, and K. Lee, "Predictive pipelined decoding: A compute-latency trade-off for exact llm decoding," 2023.

[15] B. Tadych, "Distributed llama - distributed inference of large language models with slow synchronization over ethernet." https://github.com/b4rtaz/distributed-llama/blob/main/report/report.pdf, 2024.

[16] T. Schuster, A. Fisch, J. Gupta, M. Dehghani, D. Bahri, V. Q. Tran, Y. Tay, and D. Metzler, "Confident adaptive language modeling," 2022.

[17] M. Elbayad, J. Gu, E. Grave, and M. Auli, "Depth-adaptive transformer," 2020.

[18] N. Varshney, A. Chatterjee, M. Parmar, and C. Baral, "Accelerating llama inference by enabling intermediate layer decoding via instruction tuning with lite," 2023.

[19] J. Lin, J. Tang, H. Tang, S. Yang, X. Dang, C. Gan, and S. Han, "Awq: Activation-aware weight quantization for llm compression and acceleration," 2023.

[20] J. Chee, Y. Cai, V. Kuleshov, and C. M. De Sa, "Quip: 2-bit quantization of large language models with guarantees," in *Advances in Neural Information Processing Systems* (A. Oh, T. Neumann, A. Globerson, K. Saenko, M. Hardt, and S. Levine, eds.), vol. 36, pp. 4396–4429, Curran Associates, Inc., 2023.

[21] E. Frantar and D. Alistarh, "Sparsegpt: Massive language models can be accurately pruned in one-shot," 2023.

[22] M. Kurtz, J. Kopinsky, R. Gelashvili, A. Matveev, J. Carr, M. Goin, W. Leiserson, S. Moore, B. Nell, N. Shavit, and D. Alistarh, "Inducing and exploiting activation sparsity for fast inference on deep neural networks," in *Proceedings of the 37th International Conference on Machine Learning* (H. D. III and A. Singh, eds.), vol. 119 of *Proceedings of Machine Learning Research*, (Virtual), pp. 5533–5543, PMLR, 13–18 Jul 2020.

[23] S. Kim, C. Hooper, A. Gholami, Z. Dong, X. Li, S. Shen, M. W. Mahoney, and K. Keutzer, "Squeezellm: Dense-and-sparse quantization," 2024.

[24] Message Passing Interface Forum, *MPI: A Message-Passing Interface Standard Version 4.1*, Nov. 2023.

[25] E. Hartford, "dolphin-2.1-70b." https://huggingface.co/cognitivecomputations/dolphin-2.1-70b, 2023.

[26] J. Zhao, "Tinyllama-1.1b-1t-openorca." https://huggingface.co/jeff31415/TinyLlama-1.1B-1T-OpenOrca, 2023.

[27] A. Mitra, L. D. Corro, S. Mahajan, A. Codas, C. Simoes, S. Agarwal, X. Chen, A. Razdaibiedina, E. Jones, K. Aggarwal, H. Palangi, G. Zheng, C. Rosset, H. Khanpour, and A. Awadallah, "Orca 2: Teaching small language models how to reason," 2023.

[28] A. Dale, "Goliath 120b." https://huggingface.co/alpindale/goliath-120b, 2023.

[29] X.-L. Team, "Xwin-lm," 9 2023.

[30] E. Almazrouei, H. Alobeidli, A. Alshamsi, A. Cappelli, R. Cojocaru, M. Debbah, Étienne Goffinet, D. Hesslow, J. Launay, Q. Malartic, D. Mazzotta, B. Noune, B. Pannier, and G. Penedo, "The falcon series of open language models," 2023.

[31] S. Merity, C. Xiong, J. Bradbury, and R. Socher, "Pointer sentinel mixture models," 2016.

[32] A. Cahalan, *pmap(1) Linux User's Manual*, 2002.

[33] S. Research, "Senku-70b." https://huggingface.co/ShinojiResearch/Senku-70B, 2024.

[34] J. Bai, S. Bai, Y. Chu, Z. Cui, K. Dang, X. Deng, Y. Fan, W. Ge, Y. Han, F. Huang, B. Hui, L. Ji, M. Li, J. Lin, R. Lin, D. Liu, G. Liu, C. Lu, K. Lu, J. Ma, R. Men, X. Ren, X. Ren, C. Tan, S. Tan, J. Tu, P. Wang, S. Wang, W. Wang, S. Wu, B. Xu, J. Xu, A. Yang, H. Yang, J. Yang, S. Yang, Y. Yao, B. Yu, H. Yuan, Z. Yuan, J. Zhang, X. Zhang, Y. Zhang, Z. Zhang, C. Zhou, J. Zhou, X. Zhou, and T. Zhu, "Qwen technical report," 2023.

[35] . AI, :, A. Young, B. Chen, C. Li, C. Huang, G. Zhang, G. Zhang, H. Li, J. Zhu, J. Chen, J. Chang, K. Yu, P. Liu, Q. Liu, S. Yue, S. Yang, S. Yang, T. Yu, W. Xie, W. Huang, X. Hu, X. Ren, X. Niu, P. Nie, Y. Xu, Y. Liu, Y. Wang, Y. Cai, Z. Gu, Z. Liu, and Z. Dai, "Yi: Open foundation models by 01.ai," 2024.

Appendix: Artifact Description/Artifact Evaluation

Artifact Description (AD)

I. Overview of Contributions and Artifacts

A. Paper's Main Contributions

C_1 Asynchronous Speculation: Generation of the speculative trees is performed in parallel with inference of the original token.

C_2 Continuous Speculation: Speculation is performed in micro-batches opportunistically while waiting for inference runs to complete.

C_3 Early-Inference Cancellation: In-progress speculative runs can be canceled if they are deemed superfluous or guaranteed incorrect.

C_4 KV Cache Multibuffering: The KV cache slots are carefully managed to allow multiple speculative runs at once while also allowing elision of first-token generation for speculative runs.

B. Computational Artifacts

A_1 Repository:
https://github.com/AutonomicPerfectionist/PipeInfer
DOI: 10.5281/zenodo.13328929

Artifact ID	Contributions Supported	Related Paper Elements
A_1	C_1	Figure 4
	C_2	Figure 5
	C_3	Figure 6
	C_4	Figure 7

II. Artifact Identification

A. Computational Artifact A_1

Relation To Contributions

Provides the entire PipeInfer codebase, including the components from `llama.cpp` that PipeInfer builds on.

The PipeInfer LLM inference application utilizes multiple networked compute nodes to accelerate inference of large LLMs. PipeInfer is compatible with multiple different model architectures and supports many different cluster configurations.

For instance, in the Dolphin/TinyLlama inference example provided in A1 (see link), we demonstrate inference of the target Dolphin model being accelerated with the small speculative TinyLlama model.

Exact changes made to `llama.cpp` can be seen with a git diff.

Expected Results

The expected computation speed produced by running the demo inference provided in the project README.md file on a cluster of 4 dual-socket Xeon E5-2650 servers is 1.398 tokens per second. The program outputs several different speeds; the actual inference speed is the decoding speed outputted by the head node. The Time to First Token Latency is also displayed; on the same hardware, the anticipated latency is approximately 1.04 seconds. The displayed Inter-Token Latency (ITL) can be used to verify the reported speed. Memory efficiency can be calculated from the reported generation speed divided by the memory usage reported from an external tool such as pmap or htop. Ablation results can be replicated but require modifications to the artifact.

Expected Reproduction Time (in Minutes)

60-120 minutes, including model downloads, assuming a preconfigured cluster.

Artifact Setup (incl. Inputs)

Hardware: Multiple servers with multiple sockets and many memory channels are supported and recommended. The contributions of this paper are focused on CPU, but future work can extend the work to GPUs or other accelerators. Each server must be able to connect with MPI to all other servers. Supported interconnects include Ethernet and Infiniband.

Software: Server nodes must be running a Linux-based operating system. Required runtime packages are as follows:

- MPI runtime environment (OpenMPI version 4.1.2 confirmed working)
- PipeInfer, compiled with the corresponding MPI toolchain

On Debian-based systems, the required packages can be installed with the following command:

```
$ sudo apt install \
      openmpi-bin
```

Datasets / Inputs: The models used in our paper can be downloaded from the following links (compatible speculative models are listed as children of their respective target models):

- Dolphin 70B
  - TinyLlama OpenOrca 1.1B
  - Orca2
- Goliath 120B
  - XWinLM 7B
  - XWinLM 13B
- Falcon 180B
  - Falcon 7B
  - Falcon 40B

The above links host files for several different quantization levels. The specific quantizations used can be found in Table 1 of our paper.

Installation and Deployment: Compilation requires an MPI compiler along with a C++ compilation toolchain. The following packages and versions are known to work:

- OpenMPI version 4.1.2
- GCC version 12.9
- CMake version 3.22.1
- Make version 4.3

On Debian-based systems, these dependencies can be installed with the following command:

```
$ sudo apt install \
       libopenmpi-dev \
       build-essential \
       cmake
```

Artifact Execution

T_1: Building the program following the instructions above. Note that if the target cluster contains different types of machines, the program may need to be built separately on each node.

T_2: Downloading the target and compatible speculative model. Links to the download pages can be found here as well as above. Note that system performance is dependent on the selected target and speculative models.

T_3: Running inference on the target model across the target compute cluster. Detailed execution instructions can be found at this Link, and an example bash script can be found here and in the AE appendix.

The workflow dependency is as follows: $T_1 \rightarrow T_2 \rightarrow T_3$.

Artifact Analysis (incl. Outputs)

The data output from A_1 is already partially processed. The program outputs the overall speed in tokens per second, the time to first token latency in seconds, and the inter-token latency in seconds. To obtain the figures in our paper, we plotted these measurements against the particular experiment's parameters.

The artifact, however, does not directly measure and output memory usage. For that, an external tool must be used. We utilized the open-source pmap tool, which breaks down the memory usage into individual memory-mapped regions. The memory usage figures in our paper simply used the total memory as reported by `pmap -XX`.

Artifact Evaluation (AE)

A. Computational Artifact A_1

Artifact Setup (incl. Inputs)

Hardware: Multiple servers with multiple sockets and many memory channels are supported and recommended. The contributions of this paper are focused on CPU, but future work can extend the work to GPUs or other accelerators. Each server must be able to connect with MPI to all other servers. Supported interconnects include Ethernet and Infiniband.

Software: Server nodes must be running a Linux-based operating system. Required packages are as follows:

- C/C++ compiler toolchain (GCC and G++ version 11.4.0 confirmed working)
- MPI compiler and runtime environment (OpenMPI version 4.1.2 confirmed working)
- GNU Make or CMake. (Make version 4.3 and CMake version 3.22.1 confirmed working)

On Debian-based systems, the required packages can be installed with the following command:

```
$ sudo apt install \
       openmpi-bin \
       libopenmpi-dev \
       build-essential \
       cmake
```

Datasets / Inputs: The models used in our paper can be downloaded from the following links (compatible speculative models are listed as children of their respective target models):

- Dolphin 70B, Q3_K_M
  - TinyLlama OpenOrca 1.1B, Q4_K_M
  - Orca2, Q4_K_M
- Goliath 120B, Q2_K
  - XWinLM 7B, Q4_K_M
  - XWinLM 13B, Q4_K_M
- Falcon 180B, Q3_K_M
  - Falcon 7B, Q3_K_M
  - Falcon 40B, Q3_K_M

The above links host files for several different quantization levels, the quantizations used in our paper are listed next to the model name.

Installation and Deployment: PipeInfer is implemented in the `speculative` example binary. To run PipeInfer follow these steps:

- Get the Code: Clone the Git repo here.
- Install Dependencies
  Make sure you have Make or CMake installed, as well as an MPI implementation and compiler. On Debian-based systems these can be installed with the following:

```
$ sudo apt install \
    build-essential \
```

Listing 0 (Cont.):

```
cmake \
openmpi-bin \
libopenmpi-dev
```

- Build
  To build PipeInfer you have two different options:
  - Using 'make':

```
$ make speculative \
    CC=mpicc \
    CXX=mpicxx \
    LLAMA_MPI=ON \
    -j
```

  - Using 'CMake':

```
$ mkdir build
$ cd build
$ cmake .. \
    -DCMAKE_C_COMPILER=mpicc \
    -DCMAKE_CXX_COMPILER=mpicxx
    -DLLAMA_MPI=1
$ cmake \
    --build . \
    --target speculative \
    --config Release
```

  For comparisons against the sequential and speculative baselines, replace the `speculative` target in the above build commands with `main` and `speculative_orig` respectively.
  Note: For version history reasons the compilation target named `speculative` is the PipeInfer binary, while the one named `speculative_orig` is the standard speculative inference strategy binary.

Artifact Execution

T_1: Building the program following the instructions above. Note that if the target cluster contains different types of machines, the program may need to be built separately on each node.

T_2: Downloading the target and compatible speculative model. Links to the download pages can be found here as well as above. Note that system performance is dependent on the selected target and speculative models.

T_3: Running inference on the target model across the target compute cluster. An example bash script that runs experiments for a 4 node cluster can be found below.

The workflow dependency is as follows: $T_1 \rightarrow T_2 \rightarrow T_3$.

Artifact Analysis (incl. Outputs)

A_1 appends the recorded data to a `results.csv` file after each experiment. This file contains 4 columns: the prompt processing speed, the evaluation speed, the average inter-token latency, and the TTFT latency.

This data is written not only when running PipeInfer, but also when running the sequential or speculative inference binaries. Thus, one may evaluate PipeInfer by running an experiment with each of the three inference strategies and analyzing the resulting CSV file.

We have written a simple Python script called `plot.py`, included in A_1, to generate the bar charts shown in our paper. The script segments the CSV file into groups of 3 rows, one row for each of the implementation strategies. Each row within a group must have been ran with the same model. Therefore, to generate the CSV in the proper form, it is advised to run each experiment within a group in the follow order: $sequential \rightarrow speculative \rightarrow pipeinfer$.

An example script to generate results for a 4-node cluster is shown below. To run, set the environment variables `DOLPHIN_URL` and `TINYLLAMA_URL`.

Listing 1: experiments.sh

```
#!/usr/bin/env bash

cd /tmp


if ! [ -f PipeInfer ]; then
        git clone https://github.com
            /AutonomicPerfectionist/
            PipeInfer.git
fi

MODEL_DIR=/tmp/PipeInfer/models

mkdir -p $MODEL_DIR
cd $MODEL_DIR


if ! [ -f dolphin-2.2-70b.Q3_K_M.
    gguf ]; then
  wget $DOLPHIN_URL
fi

if ! [ -f tinyllama-1.1b-1t-openorca
    .Q4_K_M.gguf ]; then
  wget $TINYLLAMA_URL
fi

cd /tmp/PipeInfer
rm -rf build
mkdir -p build
cmake -S /tmp/PipeInfer -B /tmp/
    PipeInfer/build \
     -DCMAKE_C_COMPILER=mpicc \
     -DCMAKE_CXX_COMPILER=mpicxx \
```

Listing 1 (Cont.): experiments.sh

```
    -DLLAMA_MPI=1
cmake --build . --target speculative --config Release
cmake --build . --target speculative_orig --config Release
cmake --build . --target main --config Release

cd ..

rm results.csv


BIN_DIR=/tmp/PipeInfer/build/bin
PROMPT="<|im_start|>system
You are an AI based sentient companion, capable of human emotions.
You will behave like a human, but aware of your AI nature.
You will avoid speaking like an AI.
Please continue your conversation with the user.<|im_end|>
<|im_start|>user
Write a short python program demonstrating advanced features. Don't explain it.<|im_end|>
<|im_start|>assistant"

# Experiment 1
mpirun -np 4 $BIN_DIR/main \
    -md $MODEL_DIR/tinyllama-1.1b-1t-openorca.Q4_K_M.gguf \
    -m $MODEL_DIR/dolphin-2.2-70b.Q3_K_M.gguf \
    -e \
    -p "$PROMPT" \
    -n 128 \
    --mpi-layer-split 0.25,0.25,0.25,0.25 \
    --ignore-eos \
    --temp -1.0 \
    --repeat-last-n 0 \
    --draft 4 \
    -c 1024 \
    -pa 0.001 \
    -ps 0.8 \
    --numa \
    -pr 0.4 \
    -pd 0.01 \
    -np 3

# Experiment 2: speculative
mpirun -np 4 $BIN_DIR/speculative_orig \
    -md $MODEL_DIR/tinyllama-1.1b-1t-openorca.Q4_K_M.gguf \
    -m $MODEL_DIR/dolphin-2.2-70b.Q3_K_M.gguf \
    -e \
    -p "$PROMPT" \
    -n 128 \
    --mpi-layer-split 0.1,0.4,0.5/1.0 \
    --ignore-eos \
    --temp -1.0 \
    --repeat-last-n 0 \
    --draft 4 \
    -c 1024 \
    -pa 0.001 \
    -ps 0.8 \
    --numa \
    -pr 0.4 \
    -pd 0.01 \
    -np 3

# Experiment 3: PipeInfer
mpirun -np 4 $BIN_DIR/speculative \
    -md $MODEL_DIR/tinyllama-1.1b-1t-openorca.Q4_K_M.gguf \
    -m $MODEL_DIR/dolphin-2.2-70b.Q3_K_M.gguf \
    -e \
    -p "$PROMPT_FILE" \
    -n 128 \
    --mpi-layer-split 0.1,0.4,0.5/1.0 \
    --ignore-eos \
    --temp -1.0 \
    --repeat-last-n 0 \
    --draft 4 \
    -c 1024 \
    -pa 0.001 \
    -ps 0.8 \
    --numa \
    -pr 0.4 \
    -pd 0.01 \
    -np 3

python3 /tmp/PipeInfer/plot.py
```

Examples of expected evaluation results are shown in Figures 1, 2, and 3.

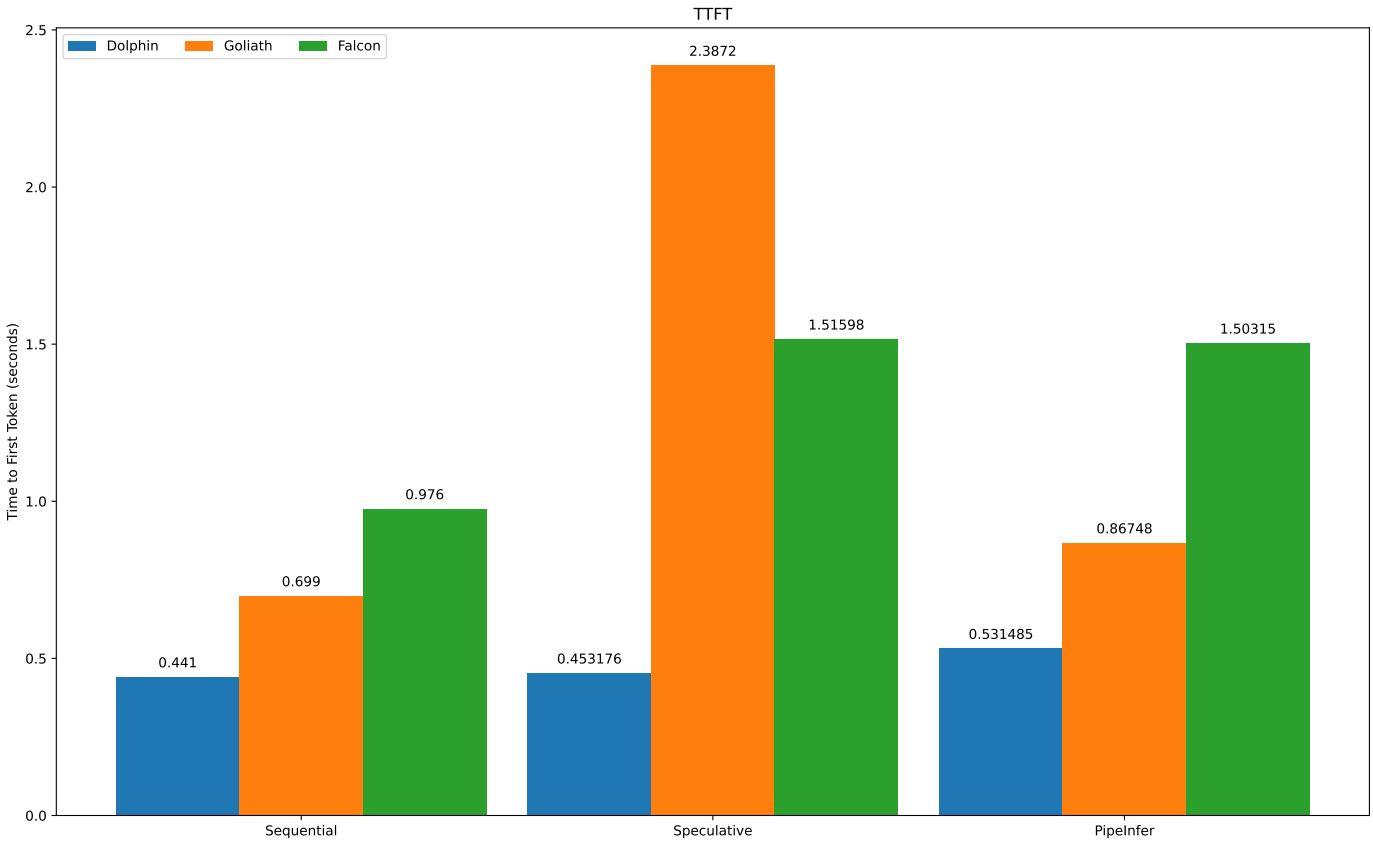

Fig. 1: Time-to-first-token latency

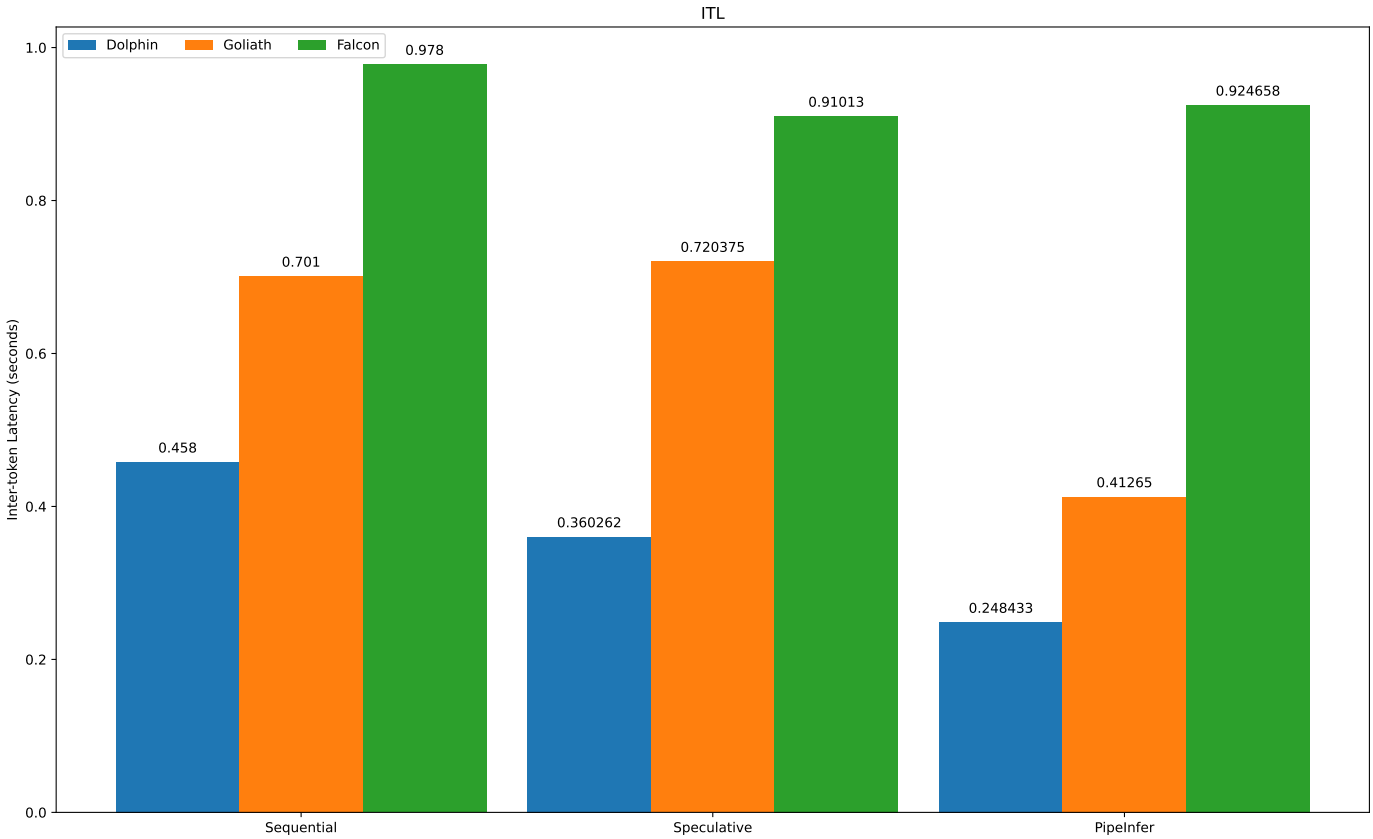

Fig. 2: Inter-token latency

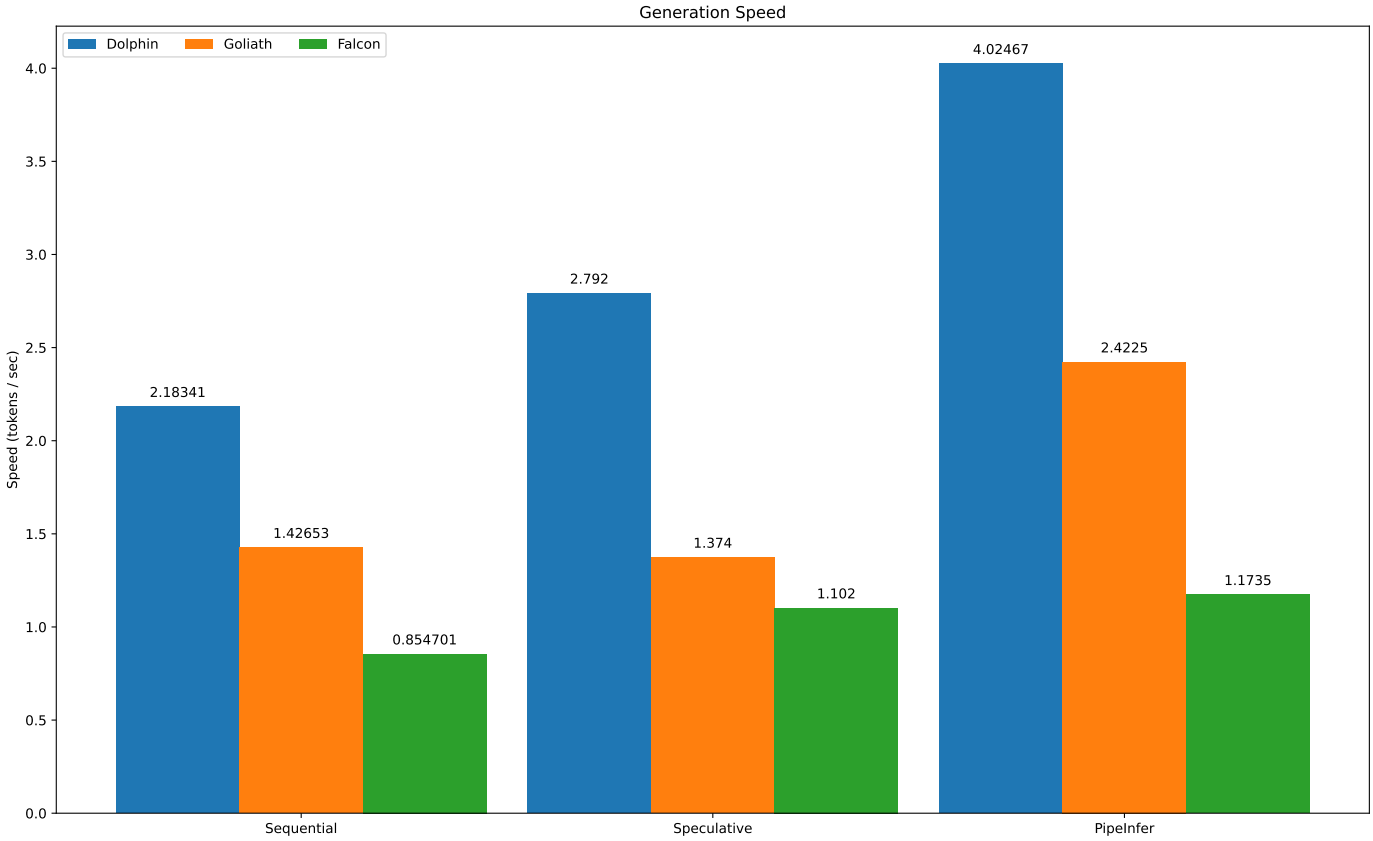

Fig. 3: Generation speeds.